Hindawi
Complexity
Volume 2021, Article ID 6697923, 14 pages
https://doi.org/10.1155/2021/6697923

Research Article

Investigation of ANN Architecture for Predicting Load-Carrying Capacity of Castellated Steel Beams

Thuy-Anh Nguyen, Hai-Bang Ly, and Van Quan Tran

University of Transport Technology, Hanoi 100000, Vietnam

Correspondence should be addressed to Hai-Bang Ly; banglh@utt.edu.vn

Received 15 December 2020; Accepted 24 May 2021; Published 30 May 2021

Academic Editor: Haitham Afan

Castellated steel beams (CSB) are an attractive option for the steel construction industry thanks to outstanding advantages, such as the ability to exceed large span, lightweight, and allowing flexible arrangement of the technical pipes through beams. In addition, the complex localized and global failures characterizing these structural members have led researchers to focus on the development of efficient design guidelines. This paper aims to propose an artificial neural network (ANN) model with optimal architecture to predict the load-carrying capacity of CSB with a scheme of the simple beam bearing load located at the center of the beam. The ANN model is built with 9 input variables, which are essential parameters equivalent to the geometrical properties and mechanical properties of the material, such as the overall depth of the castellated beam, the vertical projection of the inclined side of the opening, the web thickness, the flange width, the flange thickness, the width of web post at middepth, the horizontal projection of inclined side of the opening, the minimum web yield stress, and the minimum flange yield stress. The output variable is the load-carrying capacity of the CSB. With the optimal ANN architecture [9-1-1] containing one hidden layer, the performance of the ANN model is evaluated based on statistical criteria such as R^2, RMSE, and MAE. The results show that the optimal ANN model is a highly effective predictor of the load-carrying capacity of the CSB with the best value of $R^2 = 0.989$, RMSE = 3.328, and MAE = 2.620 for the testing part. The ANN model seems to be the best algorithm of machine learning for predicting the CSB load-carrying capacity.

1. Introduction

In modern construction, steel structures are used for abundant structures, including heavy industrial buildings, high-rise buildings, equipment support systems, infrastructure, bridges, towers, and racking systems [1]. The steel structure has numerous advantages such as large bearing capacity thanks to the high strength steel material, high reliability thanks to the uniform material, and the elastic and ductile capacity of steel, making it easy to transport and assemble [2]. Due to the high cost of steel, many structural engineers have worked hard to find ways to reduce costs for steel structures [3, 4]. Therefore, several solutions have been proposed to increase the rigidity or load capacity of the structure without increasing the weight of steel. Castellated steel beams (CSB) with web openings are among the first suggestions of these solutions [5]. This type of beam is made from wide flange I-beams, then cutting the belly plate in a zigzag line, welding the two halves on top of each other, and welding by vertical welding seams along the beam [3, 4, 6, 7]. This increases the section height but does not increase weight compared to the original solid beam; thus, bending resistance characteristics such as the moment of inertia, section modulus, and the radius of inertia are higher, and the beam stiffness and flexural resistance of sections are enhanced [3, 7, 8]. Therefore, the beam bearing capacity increases, the deflection is small, and the beam is able to exceed the large aperture [7].

However, the web openings will change the stress distribution on the bending sections [4]. Near the web openings, the stress distribution is quite complex, and stress concentration occurs. Moreover, due to the bending

moment effect, this area is also subjected to the torsion force [9]. Therefore, the critical loads of the structures are changed compared with the conventional beam [5]. So far, many experimental investigations, as well as numerical analyses, have been carried out to determine the behavior of the castellated beams under different loads. The beam failure is caused by numerous damage caused by overall bending, Vierendeel mechanism formation, welded joint rupture in the web, web post shear bucking, and web post-compression buckling [10–13]. The damage is affected by numerous factors, including geometrical dimensions of beams, loading type, and position, beam boundary conditions, material properties, as well as the distribution of residual stresses and geometric imperfections [14, 15]. Konstantinos and Mello [16] investigated the CSB behavior with close web openings by studying seven experimental samples and fourteen numerical simulation samples. The aim is to study the effects of different hole shapes and sizes on the bearing capacity and critical load of the CSB. The CSB finite element models with hexagonal and circular web openings are developed and analyzed using ANSYS. The results are compared with seven experiments test samples, thereby proposing an experimental formula to predict the load capacity of castellated beams. A numerical model studies the behavior of CSB with hexagonal and octagonal web openings up to failure developed by Soltani et al. [17]. The main purpose is to study and determine the instability in the position of web openings. In the work of Jamadar and Kumbhar [18], the authors used finite element models to determine the optimal hole size for CSB. In general, the numerical approach or laboratory experiments can only be applied to a limited number of cases, not enough to apply for general web openings beams. Furthermore, the cost of the experiment is high and requires a considerable amount of time [5]. Therefore, it is necessary to develop an efficient and universal model to study the behavior of CSB or estimate the load-carrying capacity of the CSB.

In recent years, with the rapid development of artificial intelligence technology, machine learning algorithms have been popularized in all areas of life [19–21]. Among AI algorithms, ANN is currently effective algorithms to simulate complex technical problems [22, 23]. ANN model is capable of solving complex, nonlinear problems, especially in problems where the relationship between the inputs and outputs cannot be established explicitly. An outstanding advantage of the neural network algorithm is the ability to self-study and adjust the weights. Thus, the calculation results are consistent without depending on mechanical equations, physical chemistry, or subjective opinion. Many complex problems related to structural engineering [24–26], geotechnical engineering [26–28], and materials science [29–31] have been successfully solved. In detail, Abdalla et al. [27] successfully predicted the minimum factor of safety against slope failure in clayey soils using the ANN model. The mechanical properties of FRP concrete are also predicted by the ANN model with high accuracy [32, 33]. In the field of calculating steel beams using neural networks, a number of studies have been published, such as the study of Guzelbey et al. [34] and Fonseca et al. [35]. In these studies, a backpropagation (BP) neural network is used to predict the load-carrying capacity of steel beams. The results show that the BP network is more accurate than the numerical result, practical and fast, compared to the FE model. Recently, Amayreh and Saka [36] and Gholizadeh et al. [37] used ANN to predict load failure of the CSB. In the study of Amayreh and Saka, 47 experimental data are collected, the ANN model is built with 8 input parameters, the predicted results are compared with the Blodgett method, and BS Code shows the neural network provides an effective alternative to predicting the failure loads of CSB. In the investigation of Gholizadeh et al., 140 finite element models of the web post are analyzed with 7 input parameters related to geometry size. The BP networks and ANFIS are used to predict the load-carrying capacity of the CSB. The results show that the machine learning method provides better accuracy than the equations proposed in the document. Besides, methods such as genetic algorithm (GP) and an integrated search algorithm of genetic programming and simulated annealing (GSA) are also used to predict the load-carrying capacity of the CSB. The efficiency of the ANN model shows that it is an excellent choice to develop a numerical tool for engineers to predict the loading carrying capacity of CSB, which could help to reduce experimental time consumption and cost. Therefore, the main purpose of this investigation is to propose an efficient ANN model with a more general number of input parameters and to increase the accuracy in predicting the load-carrying capacity of the CSB.

In this work, the ANN model's performance will be studied to predict the load-carrying capacity of the CSB. One of the factors affecting the model performance is to finely determine the ANN architecture. Therefore, the first goal of this work is to identify and optimize the ANN architecture to predict the load-carrying capacity of CSB. To achieve this goal, 500 simulations taking into account a data random sampling effect are performed for each model to verify the convergence and feasibility of the proposed model by Monte Carlo simulation (MSC). Then, with the optimal ANN architecture, the performance evaluation of the model is performed based on three statistical criteria, including the Coefficient of Determination (R^2), Mean Absolute Error (MAE), and Root Mean Square Error (RMSE).

2. Significance of the Research Study

Accurately predicting the load-carrying capacity of the CSB is of crucial importance because of many possible advantages and contributions to construction design. Available numerical or experimental approaches in the literature still face several limitations, for instance, the limitation of data (Amayreh and Saka [36] with 47 samples; Gholizadeh et al. [37] with 140 samples; Gandomi et al. [38] with 47 samples; and Aminian et al. [39] with 142 samples), accuracy evaluation of the ANN model, or comparison with different prediction results in the literature. Thereby, the contribution of the present investigation could be highlighted via the following ideas:

(1) The largest dataset, to the best of the author's knowledge, is used for the construction of ANN models, including 150 experimental results

(2) The reliability of ANN models is evaluated by Monte Carlo simulations

(3) The best ANN architecture is determined by the performance evaluation of 240 ANN architectures, including 15 architectures using one hidden layer, and 225 architectures with two hidden layers

(4) The performance of the best ANN architecture is compared with four studies published in the literature and confirmed the highest accuracy of the proposed ANN model in the present study

3. Database Construction

To construct a model to predict the load capacity of the CSB, a database of 150 experimental data is collected, in which 140 beam samples are simulated from the validated finite element model introduced in document [37], and 10 beam samples are tested directly for bearing capacity published in document [13]. The beams are simulated and tested under concentrated loads placed in the center of the beam until failure. The basic parameters determining the beam failure load equivalent to the nine input variables and one output variable used in this study are as follows.

Seven parameters related to the size of the CSB are used: the overall depth of castellated beam (I_1, mm); the vertical projection of inclined side of opening (I_2, mm); the web thickness (I_3, mm); the flange width (I_4, mm); the flange thickness (I_5, mm); the width of web post at mi depth (I_6, mm); the horizontal projection of inclined side of the opening (I_7, mm), where I_1 varies from 180.00 mm to 550.00 mm (mean of 335.92 mm and standard deviation of 99.60 mm), I_2 ranges from 50.00 mm to 250.00 mm (mean of 103.36 mm and standard deviation of 40.15 mm), I_3 has values between 2.00 mm and 5.00 mm (mean value is 3.65 mm and standard deviation 0.88 mm), I_4 ranges from 58.42 mm to 78.49 mm (the mean value is 68.39 mm and standard deviation of 3.54 mm), the value of I_5 is between 3.99 mm and 6.90 mm (the mean is 5.34 mm and the standard deviation is 1.03 mm), I_6 ranges from 30.00 mm to 95.00 mm (mean 53.75 mm and standard deviation 19.26 mm), and I_7 ranges from 30.00 mm to 149.35 mm (mean value is 59.23 mm and the standard deviation is 22.75 mm). The remaining two parameters are related to the mechanical properties of the material, including the minimum web yield stress (I_8, MPa) and the minimum flange yield stress (I_9, MPa). For I_8, the value varies from 311.65 MPa to 374.40 MPa (mean is 351.36 mm and the standard deviation is 7.12 mm), and I_9 ranges from 307.52 MPa to 383.54 Mpa (mean is 350.97 mm and the standard deviation is 8.25 mm). The detailed statistical information of these variables is shown in Table 1. The geometry and dimensions of the CSB are shown in Figure 1.

The dataset is randomly divided into two subsets using a uniform distribution, in which 70% of the data (corresponding to 105 data) is used to train ANN models, and 30% of the remaining data (corresponding to 45 data) is used for model verification. This means that the control data (30%) is entirely unknown to the ANN model. Therefore, the forecasting capacity of the ANN model can be assessed objectively and most accurately through the verification section. All data are normalized to the range of [0, 1] for reducing the number of errors in processing by ANN, according to the recommendations of [40]. This process ensures that the training phase of ANN models can be carried out with functional generalization capabilities. Such proportions are expressed using the following equation:

$$\chi_{\text{scaled}} = \frac{2(\chi - \lambda)}{\mu - \chi} - 1, \tag{1}$$

where λ and μ are the minimum and maximum values of given variables and χ is the value of the variable to be scaled.

In addition, a correlation analysis between the input and output parameters is performed and shown in Figure 2. Figure 2 is created to find a linear statistical correlation between parameters in the database. Therefore, a 10×10 matrix is established, where the upper triangle represents the values of the correlation coefficient, while the lower triangle shows a scatter plot between the two related variables. The diagonal of the matrix indicates the name of the parameter. The maximum value of the correlation coefficient (R) compared to Y is calculated by 0.52 (for variable I_3), followed by 0.39 (for variable I_2), 0.28 (for variable I_4), 0.24 (for variable I_7), 0.23 (for variable I_8), 0.21 (for variable I_9), 0.12 (for variable I_6), 0.09 (for variable I_5), and 0.04 (for variable I_1).

4. Methods

4.1. Artificial Neural Network. The ANN artificial neural network is a mathematical and statistical model based on the working mechanism of the biological nervous system [41]. ANN does not attempt to simulate the delicate workings of the brain, but they try to replicate the logical activity of the brain by gathering a lot of input in the form of neurons to perform computational or cognitive processes. The purpose of ANN is to define the relationship between the input parameters and the output parameters of the model. However, ANN only uses datasets without prespecifying the math functions that determine the relationship between the input and output parameters of the model. This is an effective soft computation method to solve too complex problems compared to classical mathematics and traditional methods [42].

In this study, a feedforward neural network trained by the backpropagation algorithm is used [43]. This neural network is made up of a series of processing elements, which can be called neurons or nodes. These neurons are partially or wholly connected through weights (w_{ji}) and are divided into 3 layers: input layer, output layer, and hidden layers.

During the learning process, the backpropagation algorithm uses the gradient descent search method to adjust the connection weight. The learning process starts from the input data (the input parameter vectors are entered into the

Table 1: Summary of the input and output variables of CSB beams used in this study.

	Symbol	Unit	Min	Median	Mean	Max	StD*	SK**
The overall depth of the castellated beam	I_1	mm	180.000	380.500	335.921	550.000	99.597	−0.244
The vertical projection of inclined side of opening	I_2	mm	50.000	110.000	103.358	250.000	40.154	0.389
The web thickness	I_3	mm	2.000	3.560	3.647	5.000	0.883	−0.576
The flange width	I_4	mm	58.420	66.900	68.386	78.486	3.538	0.590
The flange thickness	I_5	mm	3.988	4.590	5.344	6.900	1.032	0.666
The width of web post at middepth	I_6	mm	30.000	50.000	53.753	95.000	19.262	0.235
The horizontal projection of inclined side of opening	I_7	mm	30.000	55.000	59.230	149.352	22.754	1.128
The minimum web yield stress	I_8	MPa	311.654	352.000	351.360	374.400	7.123	−4.195
The minimum flange yield stress	I_9	MPa	307.517	352.000	350.968	383.540	8.251	−3.137
The load-carrying capacity	Y	kN	20.370	74.068	73.524	138.880	27.676	0.251

*StD = standard deviation; **SK=skewness.

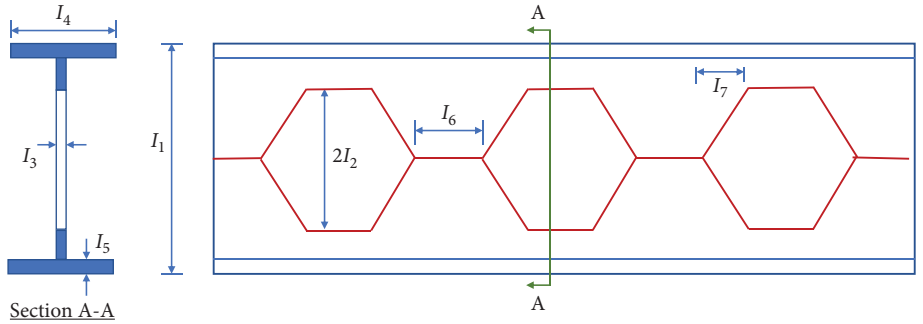

Figure 1: Castellated steel beams and opening geometry.

Figure 2: Correlation graphs between input and output variables used in this study.

input layer's neurons). At the j hidden layer neuron, the signal value received from the input layer will be composed of a total input value according to the following formula:

$$I_j = \theta_j + \sum_{i=1}^{n} w_{ji} x_i, \tag{2}$$

in which x_i are the input parameters and weights (w_{ji}) and bias (θ_j) will be randomly generated.

The pass function will then be used to calculate the output value using the following formula:

$$y_j = f\left(I_j\right). \tag{3}$$

This output value again serves as the input to the next layer neuron. As it continues, this value is passed to the neuron in the output layer. For a hidden single-layer network, this step will move to reverse propagation. The difference between the output value (y_j) and the actual value (t_j) is called the cost function, calculated as follows:

$$J = t_j - y_j. \tag{4}$$

From the cost function, compute the weight derivative of the entered and hidden classes. From there, adjust the weights and bias variables to make the predicted output of the network closer to expected:

$$\begin{aligned} \Delta w_{ji} &= \frac{\partial J}{\partial w_{ji}}, \\ \Delta \theta_j &= \frac{\partial J}{\partial \theta_j}, \\ w_{ji}(\text{new}) &= w_{ji}(\text{old}) - \eta \Delta w_{ji}, \\ \theta_j(\text{new}) &= \theta_j(\text{old}) - \eta \Delta \theta_j, \end{aligned} \tag{5}$$

where $w_{ji}(\text{new}), \theta_j(\text{new})$are weight value and bias value after adjustment; $w_{ji}(\text{old}), \theta_j(\text{old})$ are weight value and previous bias values; and η is the learning rate.

Learning speed is the optimal algorithm parameter (gradient descent). If this parameter is small, it will take many iterations for the function to reach its minimum. Conversely, if this parameter is large, the algorithm will need fewer iterations, but then it is possible that the function will ignore the minima and cannot converge.

To overcome the weights (w_{ji}) and bias values (θ_j) of the next iteration step that do not fall into a local minimum point, the momentum algorithm is used [44]. This algorithm calculates the amount of change of the variables at time t (v_t) to update the new value:

$$\begin{aligned} w_{ji}(\text{new}) &= w_{ji}(\text{old}) - \gamma v_{t-1}^{w} - \eta \Delta w_{ji}, \\ \theta_j(\text{new}) &= \theta_j(\text{old}) - \gamma v_{t-1}^{w} - \eta \Delta \theta_j, \end{aligned} \tag{6}$$

where γ is the momentum term.

With multiple hidden layers, the algorithm formulas perform the same steps. After the learning process, the model will be verified by an independent testing database.

4.2. Performance Criteria. During the training of ANN models, it is necessary to quantify the performance of the model to be able to repeat the hyperparameter adjustment to choose the best model possible. Standard quantitative performance measures for a regression model include the Coefficient of Determination (R^2), Mean Absolute Error (MAE), and Root Mean Square Error (RMSE) [45, 46]. The R^2 criterion is widely used in regression problems to estimate the correlation between the actual value and the predicted results [47]. The value of R^2 is in the range [0; 1]. In addition, RMSE and MAE measure the mean error between actual and predicted outputs [48]. Quantitatively, RMSE and MAE values are closer to 0, and the closer the value of R^2 is to 1, the more accurate the machine learning model is. The following equations represent these values:

$$\begin{aligned} R^2 &= 1 - \frac{\sum_{j=1}^{N}\left(P_j - \overline{P}_j\right)}{\sum_{j=1}^{N}\left(P_j - \overline{P}\right)}, \\ RMSE &= \sqrt{\frac{\sum_{j=1}^{N}\left(P_j - \overline{P}_j\right)^2}{N}}, \\ MAE &= \frac{\sum_{j=1}^{N}\left|P_j - \overline{P}_j\right|}{N}, \end{aligned} \tag{7}$$

in which P_j is the actual j_{th} output, $\overline{P}_j$ is the predicted j_{th} output, $\overline{P}$ is the average of the $\overline{P}_j$, and N is the number of the samples.

5. Methodology Flow Chart

The methodology of developing artificial neural networks to predict the load-carrying capacity of the CSB includes four primary steps as follows (as shown in Figure 3):

Step 1. Database preparation: in this step, a database of 140 finite element simulation beam samples and 10 direct test beam samples is collected to build the ANN model. The basic parameters to predict the load-carrying capacity of the CSB include 9 input variables divided into two groups of variables: the geometric size group and the physical properties of the material. The dataset is randomly divided into two parts, of which 70% of the data is used to train the ANN model and the remaining 30% is used to validate the built model.

Step 2. Determination of the optimum of ANN architecture: in this step, the construction of the optimum of ANN architecture based on the training dataset is carried out. The criteria used to validate the optimal ANN model include R^2, RMSE, and MAE.

Step 3. Training the optimal model: in this step, the ANN model with the optimum architecture is trained using the training dataset.

Step 4. Validating the model: in this step, the testing dataset is used to test and confirm the trained ANN model. The performance of the ANN model is evaluated by statistical criteria: R^2, RMSE, and MAE.

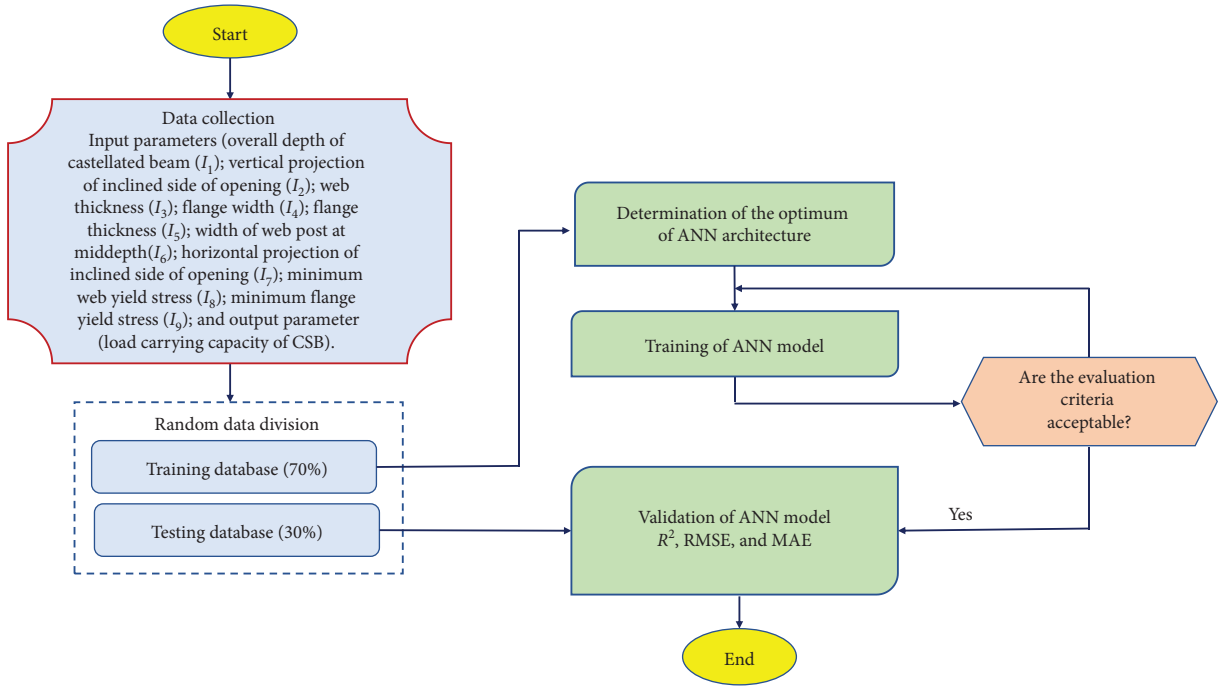

Figure 3: Methodology flowchart of the present study.

6. Results and Discussion

6.1. Investigation of Model Convergence. In this section, the determination of the ANN architecture and optimization of the ANN parameters are performed using the gradient descent algorithm. Parameters of the ANN model used in this study are given in Table 2, in which there are eight fixed parameters, and two parameters are subjected to a parametric study, namely, the number of hidden layers and the number of neurons in each hidden layer. In general, choosing the number of hidden layers and neurons in each layer is a trial-and-error test, needed to find the best configuration of the network [23]. In this study, ANN models containing one and two hidden layers are analyzed and tested. The number of neurons in each hidden layer is varied from 1 to 15. Regarding each network topology, the network training process is performed. In essence, network training is the process of adjusting the link weights and biases. These weight values are randomly taken initially, and then the network algorithm adjusts the values during the training phase. To build the network with the highest accuracy, optimization is performed with 1000 epochs to adjust the weights for each given ANN structure. In addition, in order to generalize the ANN model, 500 simulations are performed for each of the analyzed ANN structures. A total of 120,000 simulations are performed, corresponding to 15 architectures for one hidden layer and 225 architectures for two hidden layers.

The optimization process for the training and testing parts is evaluated by three statistical criteria, namely, R^2, RMSE and MAE, presented above and shown in Figure 4. Specifically, Figures 4(a), 4(c), and 4(e) represent the values of the three criteria for the training part, while Figures 4(b), 4(d), and 4(f) represent the testing part. Thanks to MCS, Figure 4 shows that, with 100 simulations, the values of the three criteria converge in about 10% of the corresponding average values. When the number of simulations increases to 400, the convergence of the ANN model improves (i.e., lower than 5% of the corresponding average values). Therefore, it could be stated that the simulations performed with 500 runs give reliable results. Overall, all investigations and results in the next sections are given by averaging the results of 500 simulations for each ANN structure.

Table 2: Summary of different ANN characteristics and investigation parameters in this study.

Parameter	Parameter	Description
Fix	Neurons in input layer	9
	Neurons in output layer	1
	Hidden layer activation function	Sigmoid
	Output layer activation function	Linear
	Cost function	Mean Square Error (MSE)
	Number of epochs	1000
	Number of simulations	500
	Training algorithm	Gradient descent
Varying	Number of hidden layers	Varying from 1 to 2
	Neurons in hidden layer	Varying from 1 to 15

6.2. Prediction Performance of Different ANN Architectures. In this section, the performance of different ANN architectures is presented to find the best ANN architecture. The performance evaluation is calculated for both the training and the testing parts by the mean and standard deviation values (StD) of the three statistical criteria (i.e., R^2, RMSE, and MAE). Figures 5(a), 5(b), and 5(c) depict the mean

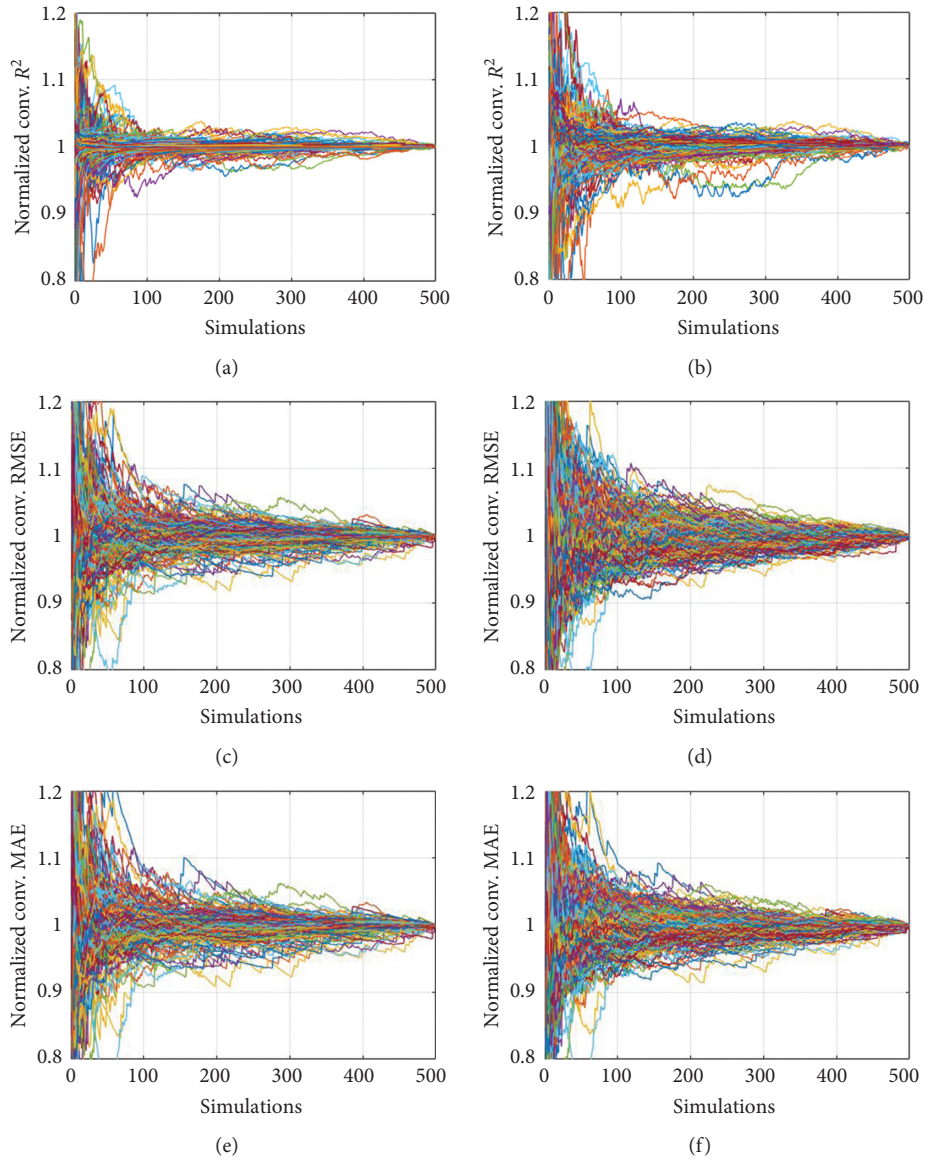

Figure 4: Convergence analysis for different ANN architecture with respect to (a) R^2 of the training parts; (b) R^2 of the testing part; (c) RMSE of the training part; (d) RMSE of the testing part; (e) MAE of the training part; and (f) MAE of the testing part.

values of R^2, RMSE, and MAE of all the analyzed ANN structures for both the training and testing parts.

In Figure 5, it worth noting that the first edge of R^2, RMSE, and MAE mean value curve is the performance of the ANN model containing 1 hidden layer, with the neuron number varying from 1 to 15. The second edge corresponds to the ANN architecture with 2 hidden layers. The first point of the second edge starts with the performance of the ANN model containing 1 neuron for the first hidden layer and 1 neuron for the second hidden layer or ANN architecture [9-1-1-1]. Each point of the remaining edges corresponds to the performance of ANN architecture containing 1 neuron in the first hidden layer, and the following points are results with 1 to 15 neurons in the second hidden layer. It means that the last point of the second edge corresponds to the performance of ANN architecture [9-1-15-1]. Overall, one edge is shown for ANN architecture containing 1 hidden layer, and 15 edges are shown for ANN architecture containing 2 hidden layers (Figure 5). Precisely, the 225 performance values of different ANN architectures can also be shown by color-map in Figures 6 and 7 for the training part and testing part, respectively. Besides, Figures 6 and 7 also show the StD values of R^2, RMSE, and MAE. Figures 6(a) and 7(a) show that the value of R^2 is relatively greater than 0.9 and 0.8 for the training and testing dataset, respectively, for ANN architectures with more than 3 neurons in the first hidden layer. Similar observations are remarked with a specific zone with low values of RMSE and MAE for both the training and testing parts (Figures 6(c), 6(e), 7(c), and 7(e)).

The performance values presented in Figure 5 show that the highest mean value of $R^2 = 0.923$ and the lowest mean values of RMSE = 7.225, MAE = 5.047 for the testing part, correspond to the ANN architecture containing 1 hidden layer [9-1-1]. Therefore, this ANN architecture has the best performance.

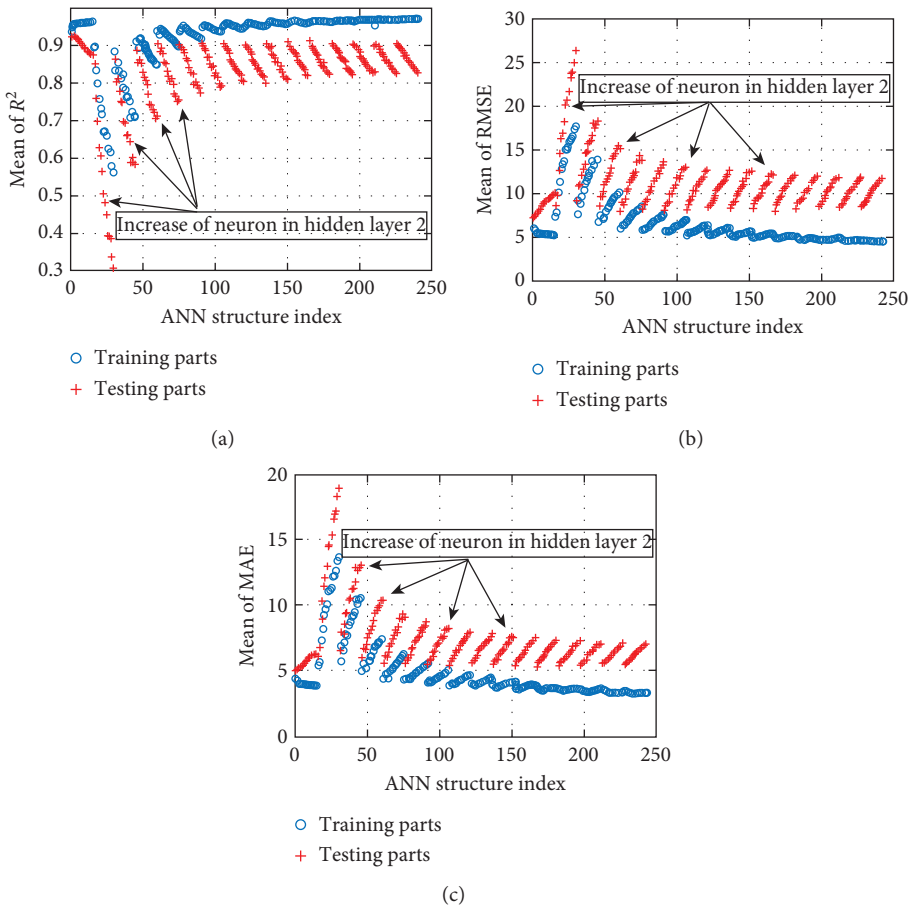

FIGURE 5: Performance of the ANN in the function of neuron number in 2 hidden layers, with respect to (a) mean value of R^2 for the training part, testing parts; (b) mean value of RMSE for the training part, testing parts; and (c) mean value of RMSE for the training part, testing parts.

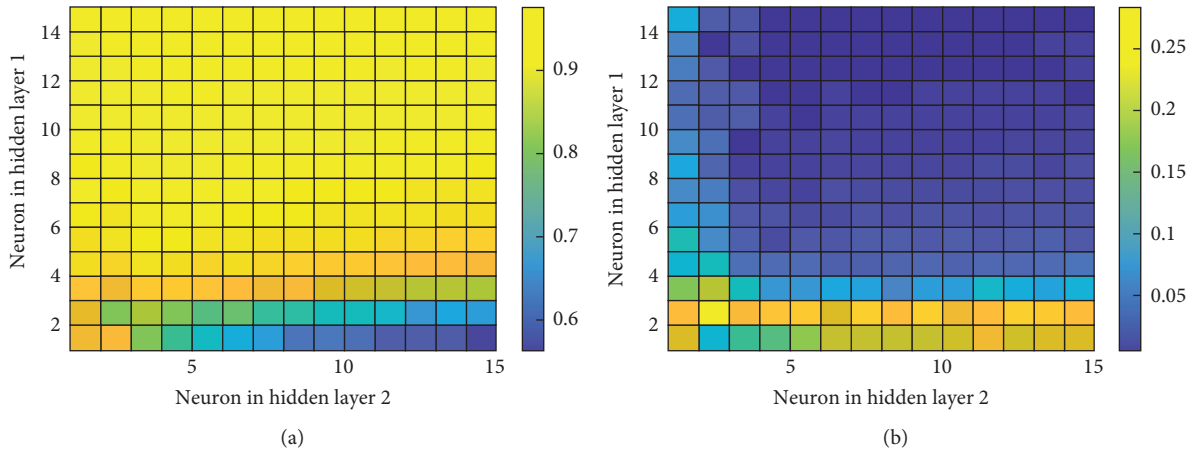

FIGURE 6: Continued.

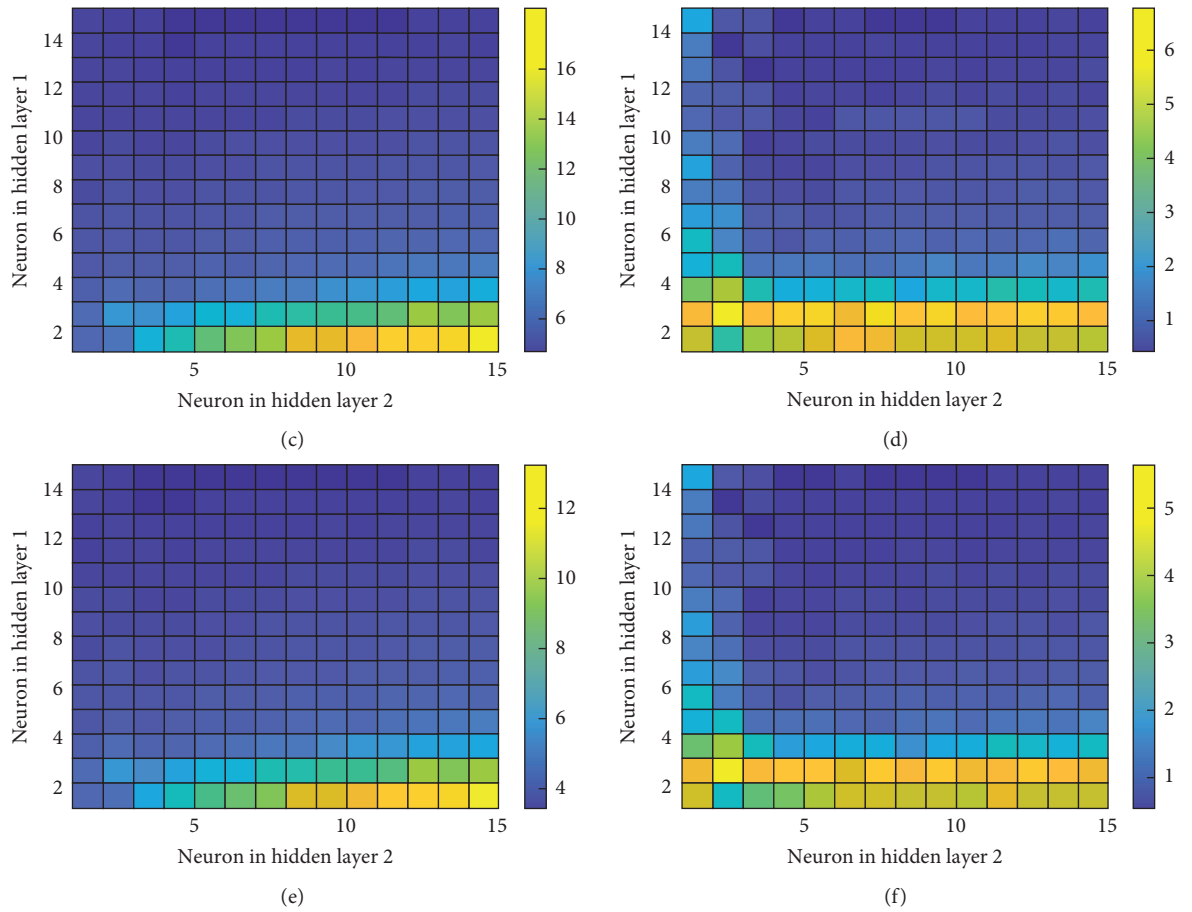

Figure 6: Color-map of ANN with 2 hidden layers in the function of the neuron of hidden layer for the training part with respect to (a) mean values of R^2; (b) StD of R^2; (c) mean of RMSE; (d) StD of RMSE; (e) mean of MAE; and (f) StD of MAE.

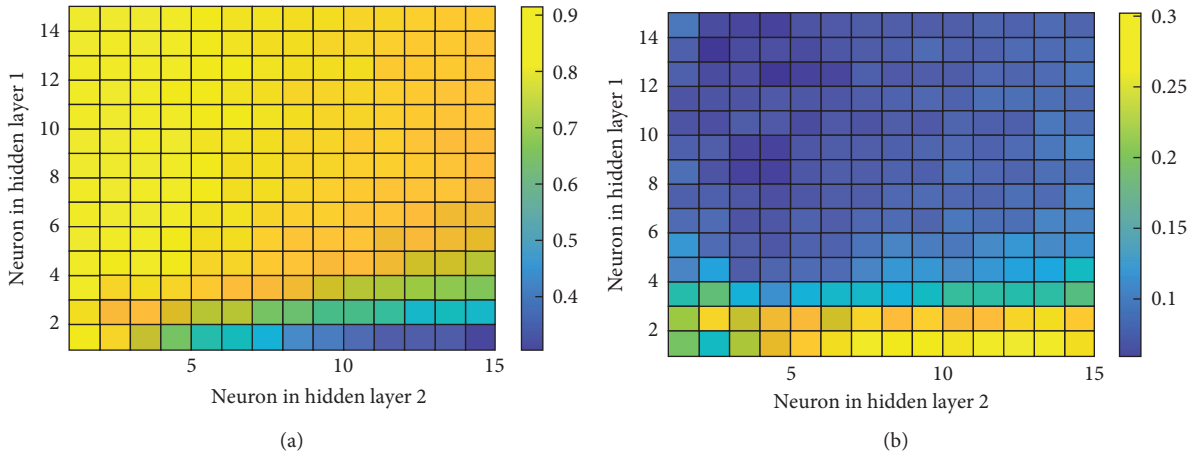

Figure 7: Continued.

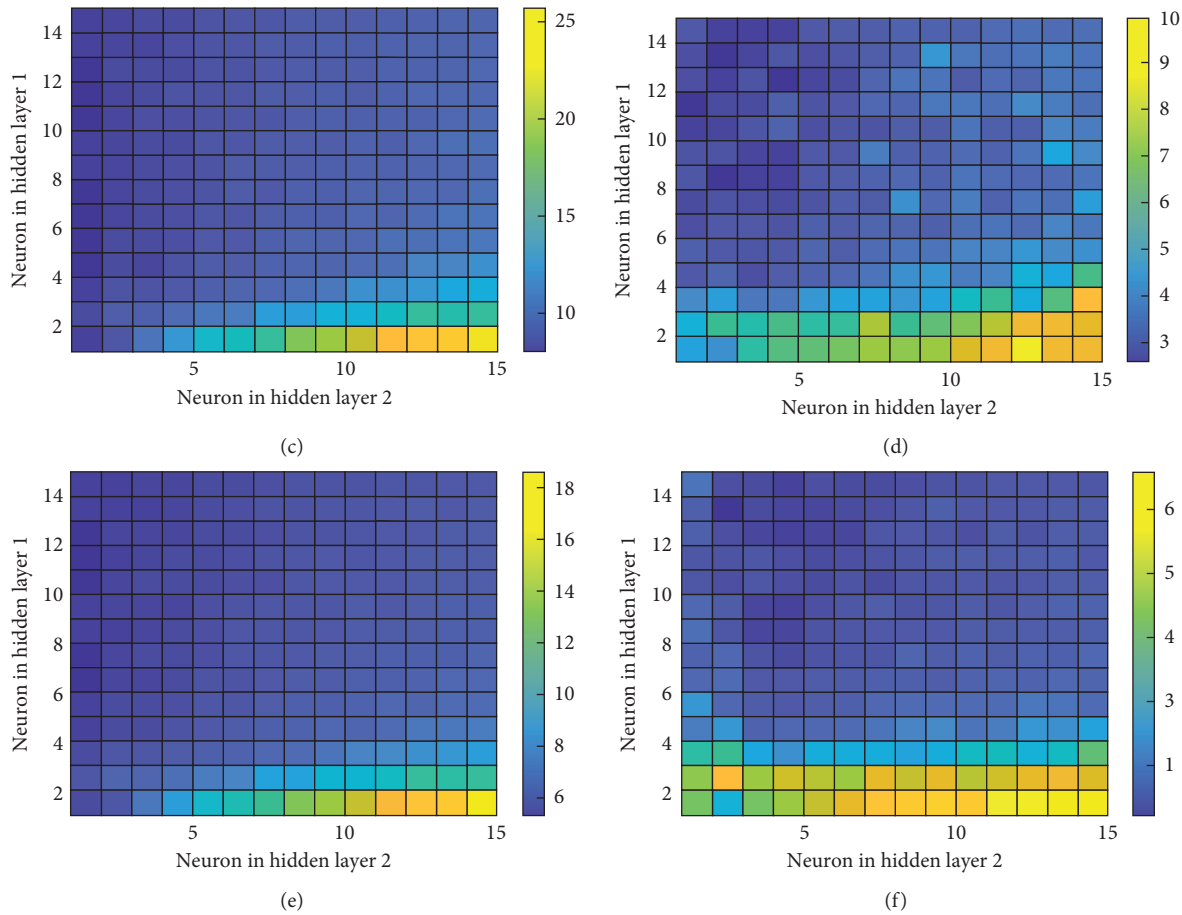

Figure 7: Color-map of ANN with 2 hidden layers in the function of neuron number of the hidden layer for the testing part with respect to (a) mean values of R^2; (b) StD of R^2; (c) mean of RMSE; (d) StD of RMSE; (e) mean of MAE; and (f) StD of MAE.

Furthermore, the results of Figures 5–7 also confirm that the ANN architecture [9-1-15-1] containing 2 hidden layers has the lowest performance, reflected by the lowest mean value of R^2, and the highest mean values of RMSE, MAE for the testing part. The lowest performance is also shown by the highest StD values of R^2, RMSE, and MAE, which means that the ANN architecture [9-1-15-1] is not stable to estimate a reliable result. Besides, with a higher neuron number of the second hidden layer, the performance of the ANN model decreases with decreasing R^2 values and increasing RMSE, MAE, and StD values. The best architecture of 2 hidden layers corresponds to the case [9-11-1-1] with performance through the mean value of R^2, RMSE, and MAE of 0.914, 7.883, and 5.233, respectively. However, these values are lower than those of the ANN architecture [9-1-1]. Therefore, such an architecture is used to predict the load-carrying capacity of CSB in the next section.

6.3. Load-Carrying Capacity Prediction of Best ANN Architecture. The optimal architecture of the ANN model is [9-1-1] applied for this section. In this section, the predictive capacity of the best performance [9-1-1] of the ANN model is presented. Specifically, the ANN architecture's prediction results [9-1-1] with the highest predictive capacity among 500 simulations are presented. The comparison between experimental critical load and predicted value by the ANN model is shown in Figure 8 for the training and testing parts. The comparison shows that the predicted values are very close to the experimental ones. The model errors are plotted between the predicted and the experimental values for the training (Figure 9(a)) and the testing parts (Figure 9(b)). The error values corresponding to the training and testing databases are small. Based on the cumulative distribution (black line), the percentage error of samples within a range can be determined. For example, with the training database, the percentage of samples with errors in the range [−5; 5] kN is about 85%. Similarly, 90% of the error of the testing set are in the range of [−5; 5] kN.

Finally, a regression model in Figures 10(a) and 10(b) shows the correlation between the actual and predicted values for the training and testing datasets, respectively. A linear fit is also applied and plotted in each case. It is observed that the linear regression lines are very close to the diagonal lines, which confirms the close correlation between the actual and predicted load-carrying capacity. The calculated values of R^2 for the training dataset and the testing dataset are 0.959 and 0.989, respectively. The values of RMSE and MAE for the training dataset are 5.405 kN and 3.718 kN. For the testing dataset, these values are 3.328 kN and 2.622 kN, respectively.

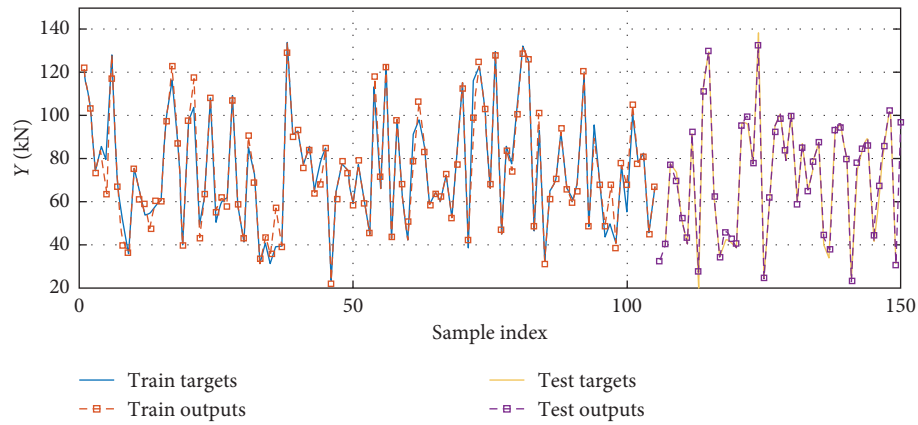

Figure 8: Experimental and predicted load-carrying capacity in function of sample index for the training and testing datasets.

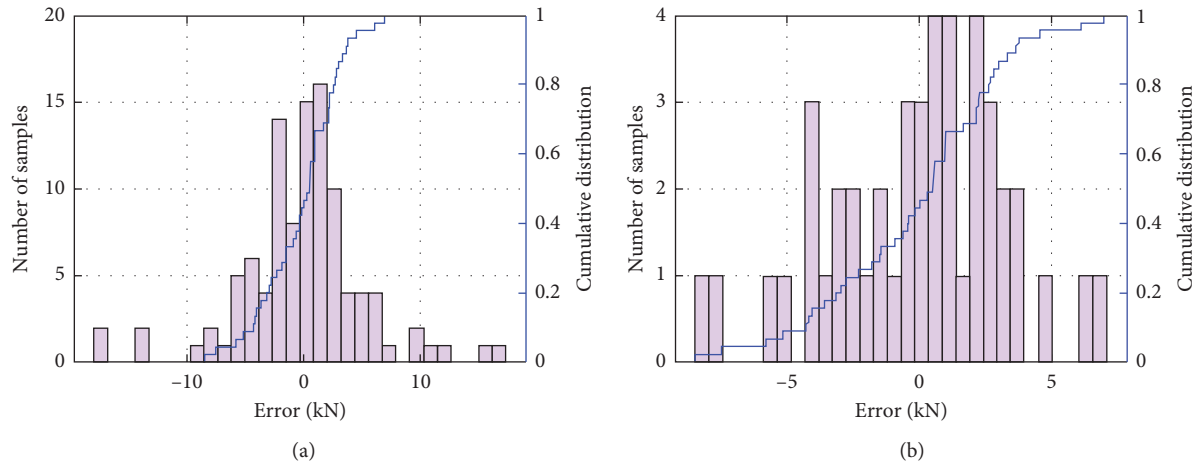

Figure 9: Experimental and predicted load-carrying capacity in function of the sample index for the training and testing datasets.

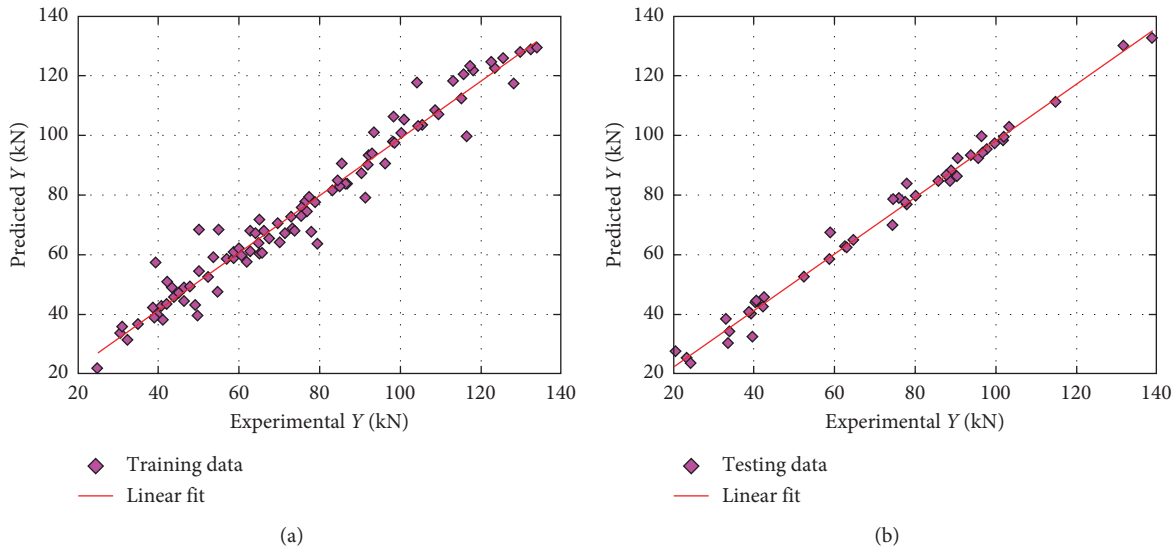

Figure 10: Regression graphs for the case of the best ANN architecture [9-1-1]: (a) training dataset and (b) testing dataset.

The results of the statistical criteria show that the ANN model with the [9-1-1] architecture can accurately predict the load-carrying capacity of the CSB.

For the sake of comparison, Table 3 shows the results of this investigation compared with different results available in the literature. For the database, the number of samples in

Table 3: Results comparison with currently popular AI techniques.

Reference	Number of data samples	Method and input	Performance criteria for testing part		
			R^2	RMSE (kN)	MAE (kN)
Amayreh and Saka [36]	47	8 inputs (minimum web yield stress, span of the castellated beam, overall depth, minimum width of the web post, web thickness, flange thickness, width of flange, loading condition) Method: backpropagation network	0.995	Not provided	Not provided
Gholizadeh et al. [37]	140	Geometrical inputs only (the overall depth of castellated beam; the vertical projection of inclined side of opening; the web thickness; the flange width; the flange thickness; the width of web post at middepth; the horizontal projection of inclined side of opening) BP1 BP2 ANFIS1 ANFIS2		4.0625 3.5611 2.7276 2.0631	
Gandomi et al. [38]	47	8 inputs (minimum web yield stress, span of the castellated beam, overall depth, minimum width of the web post, web thickness, flange thickness, width of flange, loading condition) Methods Genetic programming Least-squares regression (LSR)	 0.817 0.682	 	 32.33 36.60
Aminian et al. [39]	142	5 inputs (the overall depth of castellated beam, the vertical projection of inclined side of opening, the web thickness, the minimum web yield stress, and the width of web post at middepth) Linear genetic programming GSA algorithm	 0.960 0.952	 	 4.62 4.95
This investigation	150	9 inputs (the overall depth of castellated beam, the vertical projection of inclined side of opening, the web thickness, the flange width, the flange thickness, the width of web post at middepth, the horizontal projection of inclined side of opening, the minimum web yield stress, the minimum flange yield stress)	0.989	3.328	2.622

this investigation is the highest with 150 samples. The number of inputs for the ANN model is 9 inputs. Overall, the best ANN architecture in the present study is able to predict the load-carrying capacity of CSB with the highest accuracy, comparing with the other investigations.

7. Conclusion

This investigation aims to develop a simple but effective ANN model to predict the load-carrying capacity of CSB. To achieve this purpose, the determination of optimal ANN architecture is carried out, with two cases of hidden layers number varying from 1 to 2. Regarding each case, the neuron number in each hidden layer is varied from 1 to 15. Overall, 240 cases of ANN architectures consisting of 15 cases of 1 hidden layer and 225 cases of 2 hidden layers are proposed. Based on 150 data collected from published studies, 70% of the data are randomly selected and used for the training dataset, whereas the remaining 30% are selected for the testing dataset. A number of 500 simulations are performed for each ANN architecture. The performance of each ANN architecture is evaluated by commonly used statistical criteria, such as Determination Coefficient (R^2), Root Mean Square Error (RMSE), and Mean Absolute Error (MAE). The ANN architecture containing 1 hidden layer and 1 neuron is found as the best structure for predicting the load-carrying capacity of the CSB, with excellent agreement between model and experimental results (i.e., values of R^2, RMSE, and MAE are 0.989, 3.328, and 2.622, resp., for the testing dataset). The results of this investigation can help build a reliable soft computation tool to accurately and quickly predict the load-carrying capacity of CSB. It is important noticing that a parametric design-oriented study of CSB could be conducted in future works, thanks to the excellent accuracy of the proposed ANN model. In this case, Partial Dependence Plots analysis or parametric studies on the geometry parameters could be used to design CSB with targeted load-carrying capacity.

Data Availability

The data supporting this manuscript are from previously reported studies and datasets, which have been cited. The processed data are available from the corresponding author upon request.

Conflicts of Interest

The authors declare that they have no conflicts of interest.

References

[1] X. Zhou, Z. He, P. Chen, J. Li, and Z. Li, "Distortional buckling behavior and design consideration of castellated beams considering residual stresses," in *Proceedings of the 2019 Structural Stability Research Council Annual Stability Conference*, St Louis, MO, USA, April 2019.

[2] P. Ravi and S. Aiswarya, "Performance analysis of castellated beams with different web openings," *International Journal Of Engineering Research & Technology (IJERT)*, vol. 6, 2018.

[3] G. S. Nair and P. S. Pillai, "Review on characteristics of castellated beam," *International Research Journal of Engineering and Technology (IRJET)*, vol. 5, no. 4, pp. 3480–3484, 2018.

[4] H. W. A. Al-Thabhawee and M. A.-A. Al-Kannoon, "Improving behavior of castellated beam by adding spacer plat and steel rings," *Journal of University of Babylon for Engineering Sciences*, vol. 26, no. 4, pp. 331–344, 2018.

[5] D. K. Shendge and D. B. Shinde, "Castellated beam optimization by using finite element analysis: a review," *The International Journal of Engineering and Science*, vol. 4, pp. 12–14, 2015.

[6] B. K. Dougherty, "Castellated beams: a state of the art report," *Journal of the South African Institution of Civil Engineers*, vol. 35, no. 2, pp. 12–20, 1993.

[7] V. V. Kshirsagar and S. R. Parekar, "Behaviour of castellated beams with and without stiffeners-A review," *Behaviour*, vol. 54 pages, 2018.

[8] T. Zirakian and H. Showkati, "Distortional buckling of castellated beams," *Journal of Constructional Steel Research*, vol. 62, no. 9, pp. 863–871, 2006.

[9] S. Av and V. A. Auti, "Parametric study of castellated beam with varying depth of web opening," *International Journal of Scientific and Research Publications*, vol. 2, p. 287, 2012.

[10] A. A. Toprac and B. R. Cooke, *An Experimental Investigation of Open-Web Beams*, Welding Research Council, New York, NY, USA, 1959.

[11] M. D. Altifillisch, B. R. Cooke, and A. A. Toprac, "An investigation of open web expanded beams," *Welding Research*, vol. 22, no. 2, 1957.

[12] M. U. Hosain and W. G. Spiers, "Experiments on castellated steel beams," thesis, Department of Civil Engineering, University of Saskatchewan, Saskatoon, Canada, 1970.

[13] W. Zaarour and R. Redwood, "Web buckling in thin webbed castellated beams," *Journal of Structural Engineering*, vol. 122, no. 8, pp. 860–866, 1996.

[14] S. Elaiwi, B. Kim, and L.-Y. Li, "Bending analysis of castellated beams," *Athens Journal of Technology and Engineering*, 2018.

[15] C. H. Martins, F. P. V. Ferreira, A. Rossi, and E. V. W. Trentini, "Numerical analysis of physical and geometrical imperfections in cellular beams," *Open Journal of Civil Engineering*, vol. 7, no. 1, pp. 116–129, 2017.

[16] K. D. Tsavdaridis and C. D'Mello, "Web buckling study of the behaviour and strength of perforated steel beams with different novel web opening shapes," *Journal of Constructional Steel Research*, vol. 67, no. 10, pp. 1605–1620, 2011.

[17] M. R. Soltani, A. Bouchaïr, and M. Mimoune, "Nonlinear FE analysis of the ultimate behavior of steel castellated beams," *Journal of Constructional Steel Research*, vol. 70, pp. 101–114, 2012.

[18] A. M. Jamadar and P. D. Kumbhar, "Parametric study of castellated beam with circular and diamond shaped openings," *International Research Journal of Engineering and Technology*, vol. 2, no. 2, pp. 715–722, 2015.

[19] D. V. Dao, H. Adeli, H.-B. Ly et al., "A sensitivity and robustness analysis of GPR and ANN for high-performance concrete compressive strength prediction using a Monte Carlo simulation," *Sustainability*, vol. 12, no. 3, p. 830, 2020.

[20] H.-B. Ly, L. M. Le, H. T. Duong et al., "Hybrid artificial intelligence approaches for predicting critical buckling load of structural members under compression considering the influence of initial geometric imperfections," *Applied Sciences*, vol. 9, no. 11, p. 2258, 2019.

[21] T.-A. Nguyen, H.-B. Ly, H.-V. T. Mai, and V. Q. Tran, "Prediction of later-age concrete compressive strength using feedforward neural network," *Advances in Materials Science and Engineering*, vol. 2020, Article ID 9682740, 8 pages, 2020.

[22] M. Ahmadi, H. Naderpour, and A. Kheyroddin, "Utilization of artificial neural networks to prediction of the capacity of CCFT short columns subject to short term axial load," *Archives of Civil and Mechanical Engineering*, vol. 14, no. 3, pp. 510–517, 2014.

[23] P. B. Cachim, "Using artificial neural networks for calculation of temperatures in timber under fire loading," *Construction and Building Materials*, vol. 25, no. 11, pp. 4175–4180, 2011.

[24] Q. H. Nguyen, H.-B. Ly, V. Q. Tran et al., "A novel hybrid model based on a feedforward neural network and one step secant algorithm for prediction of load-bearing capacity of rectangular concrete-filled steel tube columns," *Molecules*, vol. 25, no. 15, p. 3486, 2020.

[25] H. Q. Nguyen, H.-B. Ly, V. Q. Tran, T.-A. Nguyen, T.-T. Le, and B. T. Pham, "Optimization of artificial intelligence system by evolutionary algorithm for prediction of axial capacity of rectangular concrete filled steel tubes under compression," *Materials*, vol. 13, no. 5, p. 1205, 2020.

[26] T. A. Pham, H.-B. Ly, V. Q. Tran, L. V. Giap, H.-L. T. Vu, and H.-A. T. Duong, "Prediction of pile axial bearing capacity using artificial neural network and random forest," *Applied Sciences*, vol. 10, no. 5, p. 1871, 2020.

[27] J. A. Abdalla, M. F. Attom, and R. Hawileh, "Prediction of minimum factor of safety against slope failure in clayey soils using artificial neural network," *Environmental Earth Sciences*, vol. 73, no. 9, pp. 5463–5477, 2015.

[28] T. A. Pham, V. Q. Tran, H.-L. T. Vu, and H.-B. Ly, "Design deep neural network architecture using a genetic algorithm for estimation of pile bearing capacity," *PLOS ONE*, vol. 15, no. 12, Article ID e0243030, 2020.

[29] D. Dao, H.-B. Ly, S. Trinh, T.-T. Le, and B. Pham, "Artificial intelligence approaches for prediction of compressive strength of geopolymer concrete," *Materials*, vol. 12, no. 6, p. 983, 2019.

[30] H.-B. Ly, B. T. Pham, D. V. Dao, V. M. Le, L. M. Le, and T.-T. Le, "Improvement of ANFIS model for prediction of compressive strength of manufactured sand concrete," *Applied Sciences*, vol. 9, no. 18, p. 3841, 2019.

[31] D. Dao, S. Trinh, H.-B. Ly, and B. Pham, "Prediction of compressive strength of geopolymer concrete using entirely steel slag aggregates: novel hybrid artificial intelligence approaches," *Applied Sciences*, vol. 9, no. 6, p. 1113, 2019.

[32] J. A. Abdalla, R. Hawileh, and A. Al-Tamimi, "Prediction of FRP-concrete ultimate bond strength using Artificial Neural Network," in *Proceedings of the 2011 Fourth International Conference on Modeling, Simulation and Applied Optimization*, pp. 1–4, Kuala Lumbur, Malaysia, April 2011.

[33] O. Abuodeh, J. A. Abdalla, and R. A. Hawileh, "Predicting the shear capacity of FRP in shear strengthened RC beams using ANN and NID," in *Proceedings of the 2019 8th International*

Conference on Modeling Simulation and Applied Optimization (ICMSAO), pp. 1–5, Manama, Bahrain, April 2019.

[34] I. H. Guzelbey, A. Cevik, and M. T. Gögüş, "Prediction of rotation capacity of wide flange beams using neural networks," *Journal of Constructional Steel Research*, vol. 62, no. 10, pp. 950–961, 2006.

[35] E. T. Fonseca, P. da S. Vellasco, S. A. L. De Andrade, and M. Vellasco, "Neural network evaluation of steel beam patch load capacity," *Advances in Engineering Software*, vol. 34, no. 11–12, pp. 763–772, 2003.

[36] L. Amayreh and M. P. Saka, "Failure load prediction of castellated beams using artificial neural networks," *Asian Journal of Civil Engineering*, vol. 6, no. 12, pp. 1-2, 2005.

[37] S. Gholizadeh, A. Pirmoz, and R. Attarnejad, "Assessment of load carrying capacity of castellated steel beams by neural networks," *Journal of Constructional Steel Research*, vol. 67, no. 5, pp. 770–779, 2011.

[38] A. H. Gandomi, S. M. Tabatabaei, M. H. Moradian, A. Radfar, and A. H. Alavi, "A new prediction model for the load capacity of castellated steel beams," *Journal of Constructional Steel Research*, vol. 67, no. 7, pp. 1096–1105, 2011.

[39] P. Aminian, H. Niroomand, A. H. Gandomi, A. H. Alavi, and M. Arab Esmaeili, "New design equations for assessment of load carrying capacity of castellated steel beams: a machine learning approach," *Neural Computing and Applications*, vol. 23, no. 1, pp. 119–131, 2013.

[40] I. H. Witten and E. Frank, "Data mining," *Acm Sigmod Record*, vol. 31, no. 1, pp. 76-77, 2002.

[41] Y. Du, Z. Chen, C. Zhang, and X. Cao, "Research on axial bearing capacity of rectangular concrete-filled steel tubular columns based on artificial neural networks," *Frontiers of Computer Science*, vol. 11, no. 5, pp. 863–873, 2017.

[42] S. Jegadesh and S. Jayalekshmi, "Application of artificial neural network for calculation of axial capacity of circular concrete filled steel tubular columns," *International Journal of Earth Sciences and Engineering*, vol. 8, pp. 35–42, 2015.

[43] D. E. Rumelhart, G. E. Hinton, and R. J. Williams, *Learning Internal Representations by Error Propagation*, Cognitive Science, California, CA, USA, 1985.

[44] A. Wanto, S. R. Andani, P. Poningsih, and R. Dewi, "Analysis of atandard gradient descent with GD momentum and adaptive LR for SPR prediction," 2018.

[45] T. Chai and R. R. Draxler, "Root mean square error (RMSE) or mean absolute error (MAE)? - arguments against avoiding RMSE in the literature," *Geoscientific Model Development*, vol. 7, no. 3, pp. 1247–1250, 2014.

[46] P. N. Chatur, A. R. Khobragade, and D. S. Asudani, "Effectiveness evaluation of regression models for predictive datamining," *International Journal of Managment, IT and Engineering*, vol. 3, no. 3, pp. 465–483, 2013.

[47] S. Menard, "Coefficients of determination for multiple logistic regression analysis," *The American Statistician*, vol. 54, no. 1, pp. 17–24, 2000.

[48] C. Willmott and K. Matsuura, "Advantages of the mean absolute error (MAE) over the root mean square error (RMSE) in assessing average model performance," *Climate Research*, vol. 30, no. 1, pp. 79–82, 2005.